

## **4-(N,N-Diethylamino)benzaldehyde thiosemicarbazone as Corrosion Inhibitor for 6061 Al – 15 vol. pct. SiC(p) Composite and its Base alloy**

**Geetha Mable Pinto<sup>1</sup>, Jagannath Nayak<sup>2</sup>, A Nityananda Shetty<sup>1\*</sup>**

<sup>1</sup>*Department of Chemistry, National Institute of Technology Karnataka, Surathkal, Srinivasnagar – 575 025, (India)*

<sup>2</sup>*Department of Metallurgical and Materials Engineering, National Institute of Technology Karnataka, Surathkal, Srinivasnagar – 575 025, (India)*

### **Abstract**

The inhibitive action of 4-(N,N-diethylamino)benzaldehyde thiosemicarbazone (DEABT) on the corrosion behavior of 6061 Al -15 vol. pct. SiC(p) composite and its base alloy was studied at different temperatures in sulfuric acid medium containing varying concentrations of it, using Tafel extrapolation and AC impedance spectroscopy (EIS) techniques. Results showed that DEABT was an effective inhibitor, showing inhibition efficiency of 80 % in 0.5 M sulfuric acid. The adsorption of DEABT on both the composite and the base alloy was found to be through physisorption obeying Langmuir's adsorption isotherm. The thermodynamic parameters such as free energy of adsorption and activation parameters were calculated.

**Key Words:** Aluminum, Metal matrix composites, EIS, Polarization, Acid corrosion

### **Introduction**

Aluminum matrix composites (AMCs) have received considerable attention for military, automobile and aerospace applications because of their low density, high strength and high stiffness.<sup>(1-6)</sup> Further, the addition of ceramic reinforcements (SiC) has raised the performance limits of the Al (6061) alloys.<sup>(7)</sup> It is known that aluminum matrix composites exhibited better resistance to mechanical wear than their base alloys and hence they have specific strength for numerous weight sensitive applications.<sup>(8-9)</sup> One of the main disadvantages in the use of metal matrix composite is the influence of reinforcement on the corrosion rate. The addition of a reinforcing phase could lead to discontinuities in the film, thereby increasing the number of sites where corrosion can be initiated and thereby making the composites

more susceptible for corrosion.<sup>(8,10)</sup> However the high corrosion rates of these composites, particularly in acid media can be combated using inhibitors.<sup>(11-12)</sup> A wide variety of compounds have been used as inhibitors for aluminum and its alloys in acid media. These are mainly organic compounds containing N, S or O atoms<sup>(13-16)</sup> and critical use of these compounds in industries has also been reviewed.<sup>(17-19)</sup> Organic compounds containing both N and S atoms function as better adsorption inhibitors because of their lone pair of electrons and polar nature of the molecules.<sup>(20-21)</sup> Thiosemicarbazone and their derivatives have continued to be the subject of extensive investigation in chemistry and biology owing to their broad spectrum of anti tumor<sup>(22)</sup>, and in many other applications including corrosion inhibition of metals.<sup>(23)</sup>

The present work aims at investigating the inhibitive action of 4-(N,N-diethylamino) benzaldehyde thiosemicarbazone (DEABT) on the corrosion behavior of 6061 Al-15 vol. pct. SiC(p) composite and its base alloy in sulfuric acid solutions at different concentration levels of the acids as well as at different temperatures.

## Materials and Experimental Procedures

### Material

The experiments were performed with specimens of 6061 Al-15 vol.pct. SiC(p) composite and its base alloy in extruded rod form (extrusion ratio 30:1). The composition of the base metal 6061 Al alloy is given in Table 1. Cylindrical test coupons were cut from the rods and sealed with epoxy resin in such a way that, the areas of the composite and the base alloy, exposed to the medium were 0.95 cm<sup>2</sup> and 0.785 cm<sup>2</sup>, respectively. These coupons were polished as per standard metallographic practice, belt grinding followed by polishing on emery papers, and finally on polishing wheel using levigated alumina to obtain mirror finish. It was then degreased with acetone, washed with double distilled water and dried before immersing in the corrosion medium.

**Table 1.** Composition of the base metal Al 6061 alloy.

Element	Cu	Si	Mg	Cr	.Al
Composition (Wt.%)	0.25	0.6	1.0	0.25	Balance

### Medium

Standard solution of sulfuric acid was prepared from analytical grade (Nice) acid. The three solutions used for the study were with 0.5 M, 0.25 M and 0.05 M concentrations of sulfuric acid. Experiments were carried out using calibrated thermostat at temperatures 30 °C, 35 °C, 40 °C, 45 °C

and 50 °C ( $\pm 0.5$  °C). The inhibitive effect was studied by introducing 50 ppm to 400 ppm (0.2 mM to 1.6 mM) of DEABT into sulphuric acid solutions.

## Electrochemical Measurements

### Tafel Polarization Studies

Electrochemical measurements were carried out by using an electrochemical work station, Auto Lab 30 and GPES software. Tafel plot measurements were carried out using conventional three electrode Pyrex glass cell with platinum counter electrode and saturated calomel electrode (SCE) as reference electrode. All the values of potential are therefore referred to the SCE. Finely polished composite and base alloy specimens were exposed to corrosion medium of different concentrations of sulfuric acid at different temperatures (30 °C to 50 °C) and allowed to establish a steady state open circuit potential. The potentiodynamic current-potential curves were recorded by polarizing the specimen to -250 mV cathodically and +250 mV anodically with respect to open circuit potential (OCP) at a scan rate of 1 mV s<sup>-1</sup>.

### Electrochemical Impedance Spectroscopy Studies (EIS)

The corrosion behaviors of the specimens of the composite and the base alloy were also obtained from EIS technique using electrochemical work station, Auto Lab 30 and FRA software. In EIS technique a small amplitude ac signal of 10 mV and frequency spectrum from 100 kHz to 0.01 Hz was impressed at the OCP and impedance data were analyzed using Nyquist plots. The charge transfer resistance,  $R_t$  was extracted from the diameter of the semicircle in the Nyquist plot.

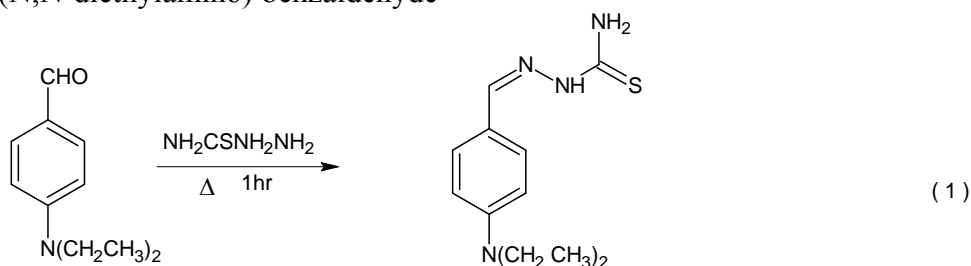
In all the above measurements, at least three similar results were considered and their average values are reported.

4-(N,N-Diethylamino)benzaldehyde thiosemicarbazone as Corrosion Inhibitor for 6061 Al – 15 vol. pct. SiC(p) Composite and its Base alloy

**Synthesis of 4 - (N, N- Diethylamino) Benzaldehyde Thiosemicarbazone**

4-(N,N-Diethylamino) benzaldehyde thiosemicarbazone (DEABT) was synthesized and recrystallised as per the reported procedure.<sup>(24)</sup> A mixture containing equimolar ethanolic 4-(N,N-diethylamino) benzaldehyde

and thiosemicarbazone were taken into a round bottom flask. The reaction mixture was refluxed on a hot water bath for about 60 minutes. The light yellow colored product obtained was separated by filtration and dried. The product was recrystallised from ethanol. The recrystallised product was checked by IR spectra, elemental analysis and melting point.



**Results and Discussion**

**Potentiodynamic Polarization (PDP) Measurements**

The polarization studies of aluminum specimens were carried out in 0.05 M – 0.5 M sulfuric acid solutions separately in the absence and in the presence of different concentrations of DEABT. Figure 1a and Figure 1b represent potentiodynamic polarization curves for the corrosion of 6061 Al – SiC composite and the base alloy,

respectively, in 0.5 M sulfuric acid solution at 30° C in the absence and in the presence of different concentrations of DEABT. Similar results were obtained in the same concentration of sulfuric acid at four other temperatures and also in the other two concentrations of the sulfuric acid at the five temperatures studied. The electrochemical parameters ( $E_{corr}$ ,  $i_{corr}$ ,  $b_a$  and  $b_c$ ) associated with the polarization measurements at different DEABT concentrations for the composite and the base alloy in three different concentrations of the sulfuric acid solution at 30° C are listed in Table 2.

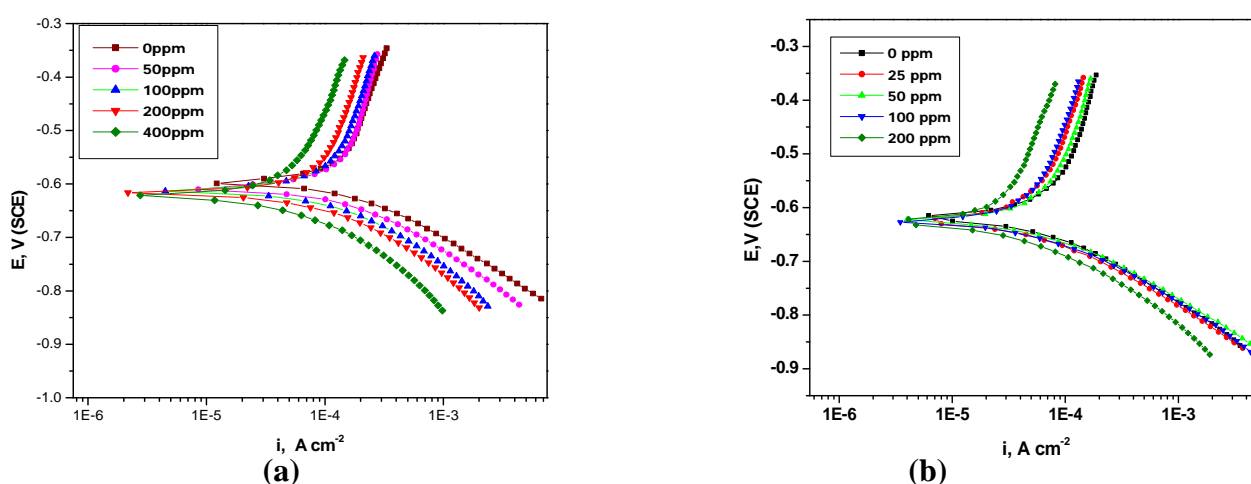


**Figure 1.** Potentiodynamic polarization curves for the corrosion of a) composite and b) base alloy in the presence of different concentrations of DEABT in 0.5 M sulfuric acid at 30°

The surface coverage  $\theta$  of the inhibitor on the metal surface is calculated by the expression

$$\theta = \frac{i_{corr(uninh)} - i_{corr(inh)}}{i_{corr(uninh)}} \quad (2)$$

The Inhibition efficiency (% IE) is calculated by the relation

$$IE (\%) = \theta \times 100 \quad (3)$$

The data in the table clearly show that the addition of DEABT decreases the corrosion rates of both the composite and the base alloy. Inhibition efficiency increases with increasing DEABT concentration. For the inhibited systems, the values of  $E_{corr}$  are shifted to more negative direction and the cathodic branches of the curves are displaced to the left. These are typical features of cathodic inhibitors, in agreement with the results obtained for other aluminum alloys.<sup>(25-27)</sup>

**Table 2.** Electrochemical parameters obtained from potentiodynamic polarization measurements For the corrosion of 6061 Al-SiC composite and the base alloy in the presence of different concentrations of DEABT at 30°C

Conc. of H <sub>2</sub> SO <sub>4</sub> (M)	Composite						Base alloy					
	Conc. of inhibitor (ppm)	$i_{cor}$ ( $\mu$ A cm <sup>-2</sup> )	$-b_c$ (mV dec <sup>-1</sup> )	$b_a$ (mV dec <sup>-1</sup> )	$E_{corr}$ (mV) (SCE)	IE (%)	Conc. of inhibitor (ppm)	$i_{cor}$ ( $\mu$ A cm <sup>-2</sup> )	$-b_c$ (mV dec <sup>-1</sup> )	$b_a$ (mV dec <sup>-1</sup> )	$E_{corr}$ (mV) (SCE)	IE (%)
0.5	0	91.4	122	59	-597		0	22.9	97	37	-605	
	50	66.9	119	60	-612	30	25	19.5	95	32	-610	14
	100	47.8	116	51	-615	47	50	17.6	97	33	-612	24
	200	36.5	115	53	-618	60	100	13.2	95	33	-617	42
	400	22.8	118	55	-622	75	200	9.9	98	32	-622	57
0.25	0	44.8	88	56	-615		0	-622	85	28	10.4	
	25	36.3	90	52	-622	25	10	-627	84	27	8.65	17
	50	26.4	93	49	-627	37	25	-630	80	26	6.59	37
	100	22.6	90	47	-633	45	50	-635	82	24	5.45	48
	200	17.7	92	46	-631	52	100	-638	81	25	4.98	55
0.05	0	25.5	70	50	-664		0	9.9	54	20	-679	
	10	20.2	72	46	-667	21	5	7.7	59	22	-685	22
	25	15.9	74	42	-669	35	10	7.1	61	25	-687	28
	50	12.3	73	44	-674	50	25	6.3	62	22	-691	36

The anodic and cathodic Tafel slopes remain almost unchanged for the uninhibited and inhibited systems. This indicates that the inhibitive action of DEABT occurs by simple blocking of the available surface area for corrosion attack.

In other words, the inhibitors decrease the surface area available for corrosion reaction, without affecting the reaction mechanism and they only cause inactivation of part of the surface.<sup>(28-29)</sup> This fact is an important observation, since the presence of

*4-(N,N-Diethylamino)benzaldehyde thiosemicarbazone as Corrosion Inhibitor for 6061 Al – 15 vol. pct. SiC(p) Composite and its Base alloy*

SiC particles in the composite initiates cathodic sites which are responsible for the higher corrosion of the composite than that of the base alloy<sup>(8,10)</sup>. Therefore blocking of these sites via DEABT adsorption would result in decreasing the corrosion rate of composite to a greater extent as compared to the base alloy. The comparison of inhibition efficiency of DEABT for the composite and base alloy at different concentrations and different temperatures shows that the inhibition effect is more on the composite than on the base alloy. The increase in the efficiency of the inhibitor in the case of composite may be due to its heterogenic nature, where the incorporation of silicon carbide acts as the potential active

site for the adsorption of the inhibitor. The increase in inhibition efficiency with increasing inhibitor concentration indicates an increase in the adsorption of inhibitor molecules on the metal surface. Thus, the surface coverage increases as the inhibitor concentration increases.

**Electrochemical Impedance spectroscopy (EIS)**

Corrosion behavior of 6061 Al- SiC composite and its base alloy in 0.05 M – 0.5 M sulfuric acid solutions, in the absence and presence of different concentrations of DEABT was also studied by electrochemical

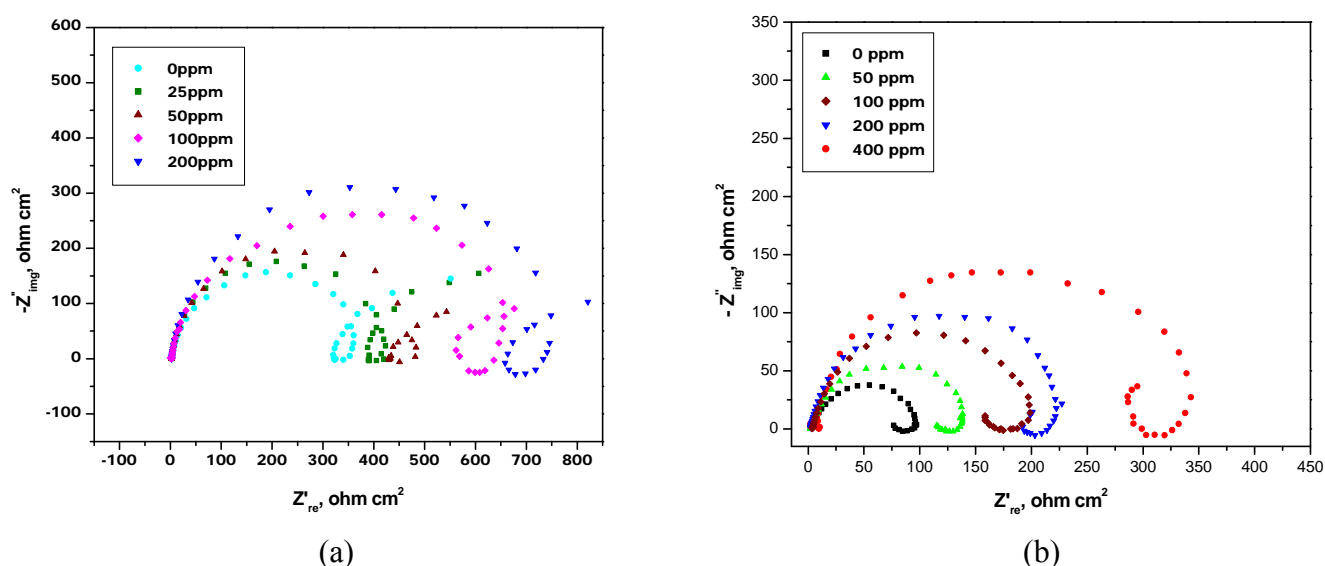


**Figure 2.** Nyquist plots for the corrosion of 6061 Al- SiC (a) composite (b) base alloy in 0.5 M sulfuric acid at 30 °C in the presence of different concentrations of DEABT.

impedance spectroscopy. Figure 2a and Figure 2b represent Nyquist plots for the corrosion of 6061 Al –SiC composite and its base alloy, respectively, in the presence of different concentrations of DEABT in 0.5 M

sulfuric acid at 30 °C. Similar results were obtained in other four temperatures of sulfuric acid. The electrochemical parameters obtained from the EIS measurements are tabulated in Table 3.

**Table 3.** Electrochemical parameters obtained from EIS measurements for the corrosion of 6061 Al-SiC composite and the base alloy in the presence of different concentrations of DEABT at 30°C

Composite					Base alloy			
Conc. of H <sub>2</sub> SO <sub>4</sub> (M)	Conc. of inhibitor r (ppm)	R <sub>t</sub> (Ω cm <sup>2</sup> )	CPE (μF cm <sup>-2</sup> )	IE (%)	Conc. of inhibitor (ppm)	R <sub>t</sub> (Ω cm <sup>2</sup> )	CPE (μF cm <sup>-2</sup> )	IE (%)
0.5	0	93.9	222		0	360.1	27.1	
	50	145.6	195	31	25	440.0	26.7	18
	100	179.3	163	48	50	505.2	25.5	29
	200	245.0	134	62	100	656.0	23.2	45
	400	378.9	117	75	200	751.3	20.1	53
0.25	0	213.0	179		0	456.7	23.4	
	25	286.8	155	25	10	559	21.2	18
	50	337.8	128	36	25	739	17.8	38
	100	393.4	110	44	50	906	16.2	50
	200	449.8	95	50	100	1056	13.3	56
0.05	0	401.0	101		0	720.0	16.7	
	10	512.3	76	29	5	919.0	14.2	21
	25	655.4	65	40	10	995.6	13.0	28
	50	798.8	56	55	25	1119.7	12.1	36

As can be seen from the Figure 2, the impedance diagrams show semicircles, indicating that the corrosion process is mainly charge transfer controlled. In the Nyquist plots for the 6061Al-SiC composite, the impedance spectra consists of a large capacitive loop at high frequencies (HF) and an inductive loop at low frequencies (LF). Similar impedance plots have been reported in literature for the corrosion of pure aluminum and aluminum alloys in various electrolytes such as sodium sulfate<sup>(30-32)</sup>, sulfuric acid<sup>(31-32)</sup>, acetic acid<sup>(31)</sup>, sodium chloride<sup>(33-34)</sup> and hydrochloric acid.<sup>(35-41)</sup> The general shape of the curve is similar for all individual samples of the base alloy, with large capacitive loop at high frequencies (HF) and an inductive loop at intermediate frequencies (IF), followed by a second capacitive loop at low frequency (LF) values. Similar results have been reported in literature for the corrosion of pure aluminum in acidic and neutral solutions.<sup>(30-31)</sup>

The high frequency capacitive loop could be assigned to the charge transfer of the corrosion process and to the formation of oxide layer<sup>(42-43)</sup>. The oxide film is considered to be a parallel circuit of a resistor due to the ionic conduction in the oxide film and a capacitor due to its dielectric properties. According to Brett<sup>(36, 38)</sup>, the capacitive loop is corresponding to the interfacial reactions, particularly, the reaction of aluminum oxidation at the metal/ oxide /electrolyte interface. The process includes the formation of Al<sup>+</sup> ions at the metal/oxide interface, and their migration through the oxide/solution interface where they are oxidized to Al<sup>3+</sup>. At the oxide/solution interface, OH<sup>-</sup> or O<sup>2-</sup> ions are also formed. The fact that all the three processes are represented by only one loop could be attributed either to the overlapping of the loops of processes, or to the assumption that one process only dominates, excluding the other processes.<sup>(34-35)</sup> The other explanation offered to the high frequency capacitive loop is the oxide film itself.

4-(*N,N*-Diethylamino)benzaldehyde thiosemicarbazone as Corrosion Inhibitor for 6061 Al – 15 vol. pct. SiC(*p*) Composite and its Base alloy

The origin of the inductive loop has often been attributed to surface or bulk relaxation of species in the oxide layer.<sup>(44)</sup> The LF inductive loop may be related to the relaxation process obtained by adsorption and incorporation of sulfate ions, oxide ions and charged intermediates on and into the oxide film.<sup>(33)</sup> The second capacitive loop observed at LF values could be assigned to the metal dissolution.<sup>(32)</sup> The measured values of polarization resistance ( $R_p$ ) increase with the increasing concentration of DEABT in the solution, indicating the decrease in the corrosion rate for the base metal with increase in DEABT concentration up to critical concentration of the inhibitor. This is in accordance with the observations obtained from potentiodynamic measurements.

However, in the case of Al/SiC composites, the obtained semicircles in absence or in presence of inhibitor are depressed. Deviation of this kind are referred to as frequency dispersion, and have been attributed to inhomogeneities of solid surfaces, as the aluminum composite is reinforced with

SiC particles. Mansfeld, *et al.*<sup>(42-43)</sup> have suggested an exponent  $n$  in the impedance function as a deviation parameter from the ideal behavior. By this suggestion, the capacitor in the equivalent circuit can be replaced by a so-called constant phase element (CPE) that is a frequency-dependent element and related to surface roughness. The impedance function of a CPE has the following equation<sup>(31)</sup>:

$$Z_{CPE} = \frac{1}{(Y_0 J \omega)^n} \quad (4)$$

where the amplitude  $Y_0$  and  $n$  are frequency independent, and  $\omega$  is the angular frequency for which  $-Z''$  reaches its maximum values,  $n$  is dependent on the surface morphology, with values,  $-1 \leq n \leq 1$ .  $Y_0$  and  $n$  can be calculated by the equations proved by Mansfeld *et al.*<sup>(42-43)</sup> In the case of base alloy, due to the homogenous surface, frequency dispersion is very less. Therefore the obtained semicircles in the impedance spectra are not depressed.

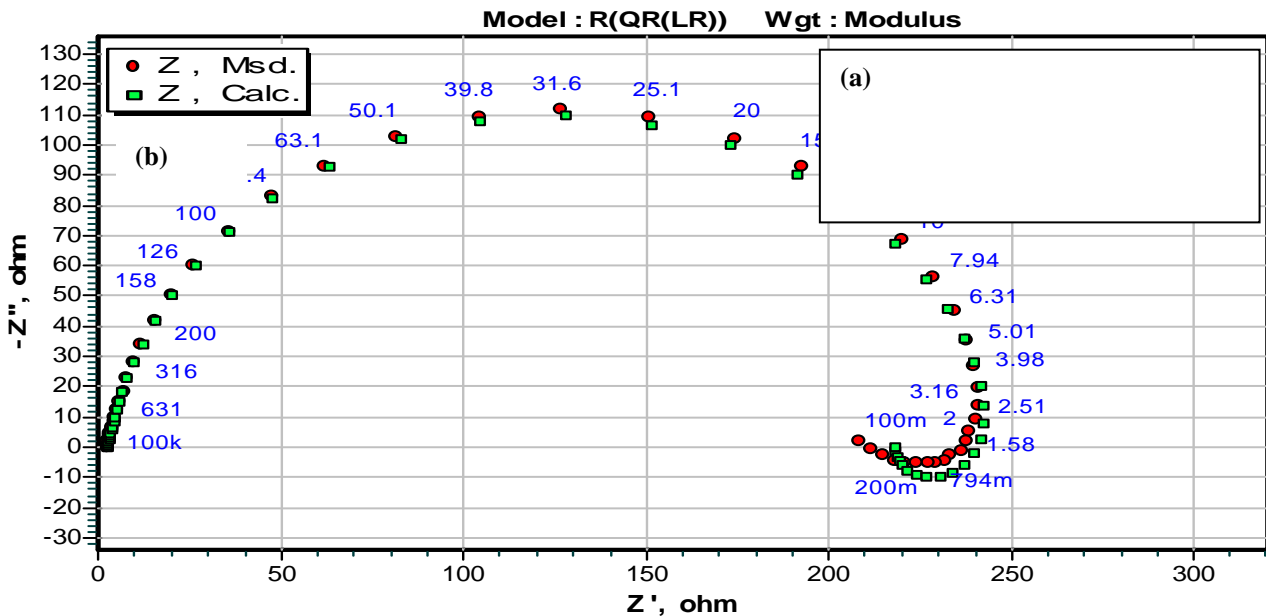


**Figure 3a.** Equivalent circuit model used to fit the experimental data of the composite

An equivalent circuit of five elements was used to simulate the measured impedance

data of the composite as shown in Figure 3a. In this equivalent circuit  $R_s$  is the solution

resistance and  $R_t$  is the charge transfer resistance.  $R_L$  and  $L$  represent the inductive elements. This also consists of constant phase element, CPE (Q) in parallel to the parallel resistors  $R_t$  and  $R_L$ , and the later is in series with the inductor  $L$ . The polarization resistance  $R_p$  can be calculated from<sup>(5)</sup>:

$$R_p = \frac{R_L \times R_t}{R_L + R_t} \quad (5)$$

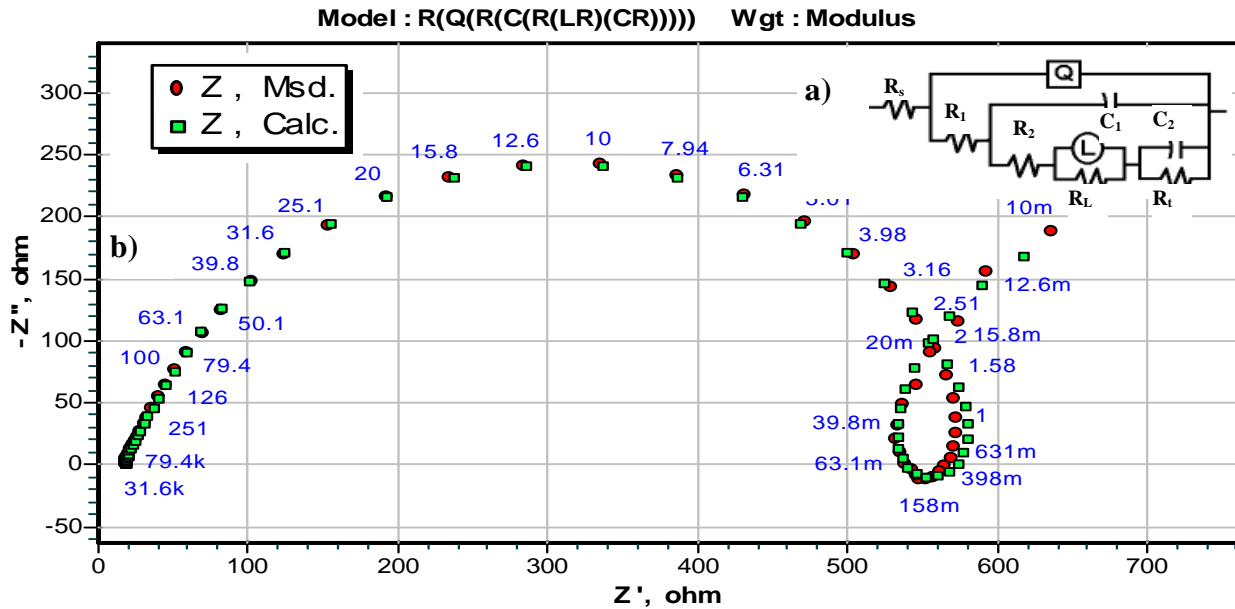


**Figure 3b.** Equivalent circuit model used to fit the experimental data of the base alloy.

An equivalent circuit of nine elements was used to simulate the measured impedance data of the base alloy as shown in Figure 3b. In this equivalent circuit  $R_s$  is the solution resistance and  $R_t$  is the charge transfer resistance.  $R_L$  and  $L$  represent the inductive elements. This also consists of constant phase element; CPE (Q) in parallel to the series capacitors  $C_1$ ,  $C_2$  and series resistors  $R_1$ ,  $R_2$ ,  $R_L$  and  $R_t$ .  $R_L$  is parallel with the inductor  $L$ . The polarization resistance  $R_p$  and double layer capacitance  $C_{dl}$  can be calculated from equations<sup>(6)</sup> and<sup>(7)</sup>:

$$R_p = R_L + R_t + R_1 + R_2 \quad (6)$$

$$C_{dl} = C_1 + C_2 \quad (7)$$

Since  $R_p$  is inversely proportional to the corrosion current and it can be used to

calculate the inhibition efficiency from the relation,

$$IE\% = \left( \frac{R_p' - R_p}{R_p'} \right) \times 100 \quad (8)$$

where  $R_p'$  and  $R_p$  are the polarization resistances in the presence and absence of inhibitors.

The Bode plots for the corrosion of 6061 Al/ SiC composite and its base alloy with and without inhibitor, obtained at OCP, are presented in Figure 4. It is apparent that, in the case of composite, the phase angle maxima are quite broad after the addition of DEABT where as

there is no significant change was observed for the base alloy.

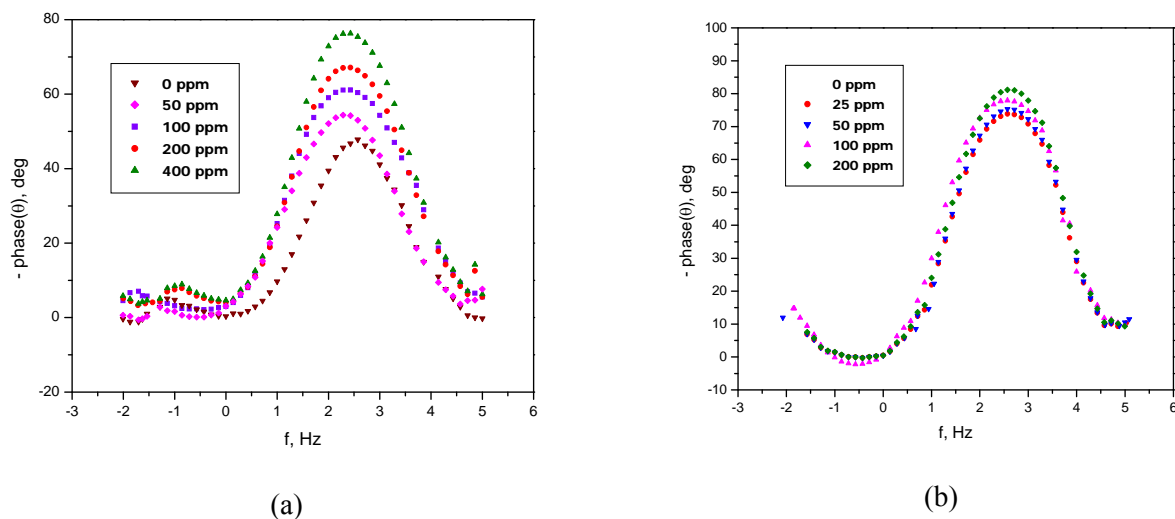


**Figure 4.** Bode plots for the corrosion of a) composite and b) base alloy in 0.5 M sulfuric acid at 30 °C in the presence of different concentrations of DEABT.

It is seen from Table 3 that  $R_s$  (solution resistance) remains almost constant, with and without the addition of DEABT for both the composite and the base alloy. It was also observed that the value of constant phase element,  $Q$ , decreases, while the values of  $R_p$  and  $R_t$  increase with the increase in the concentration of DEABT, indicating that the inhibition efficiency increases with the increase in the concentration of DEABT. The double layer between the charged metal surface and the solution is considered as an electrical capacitor. The adsorption of DEABT molecules on the aluminum surface decreases its electrical capacity because they displace the water molecules and other ions originally adsorbed on the surface. The decrease in this capacity with increase in DEABT concentrations may be attributed to the formation of a protective layer on the electrode surface. The thickness of this protective layer increases with the increase in inhibitor concentration up to their critical concentration and then decreases. The obtained CPE ( $Q$ ) value decreases

noticeably with the increase in the concentration of DEABT. In the case of composites, adsorption of negatively charged heteroatoms and  $\pi$  electrons of the benzene ring of DEABT at the Al/SiC interface occurs to a better extent than the base alloy. In the case of base alloy, due to the homogenous surface, frequency dispersion is very less. Therefore the obtained semicircles in the impedance spectra are not depressed. Significant change in the CPE values of the base alloy is not observed after the addition of an inhibitor.

A comparison of the maximum attainable inhibiting efficiencies obtained using a.c and d.c methods are listed in Table 4 for both the composite and the base alloy in 0.5 M sulfuric acid at different temperatures. The results show that the inhibition efficiencies determined by the two techniques are in good agreement. Similar levels of agreement were observed at the other two concentrations of the acid also. Though the inhibition efficiencies obtained at lower temperatures (30 °C, 35 °C, 40 °C) are quite

high, it is bit lower at higher temperatures (45 °C and 50 °C). The Tables 2, 3 and 4 also reveal that the optimum concentration of DEABT required for maximum efficiency is higher for the composite than for the base alloy. Above the optimum concentration of DEABT given in the Tables, there was no

appreciable increase in the inhibition efficiencies. The inhibition efficiencies are as high as 75% for the composite and 57% for the base alloy in 0.5 M sulfuric acid solution, but the values are 50% and 36% in 0.05 M sulfuric acid solution.

**Table 4.** Maximum inhibitor efficiencies obtained in 0.5 M sulfuric acid solution at different temperatures.

Temperature of the medium (°C)	Optimum inhibitor concentration (ppm)	Composite		Optimum inhibitor concentration (ppm)	Base alloy	
		Inhibition Efficiency (%)			Inhibition Efficiency (%)	
		Tafel method	EIS method		Tafel method	EIS method
30	400	75	74	200	56	57
35	400	70	71	200	53	54
40	400	68	69	200	51	52
45	400	59	60	200	47	49
50	400	58	59	200	44	46

#### *Effect of Temperature and Activation Parameters of Inhibition Process*

The results obtained indicate that the rates of aluminum corrosion in the absence and in the presence of DEABT increases with the increase in temperature while the inhibition efficiency decreases. This may be attributed to the higher dissolution rates of aluminum at elevated temperature and a possible desorption of adsorbed inhibitor due to the increased solution agitation resulting from higher rates of hydrogen gas evolution, which may also reduce the ability of the inhibitor to be adsorbed on the metal surface. Such behavior, observed in both the samples, suggests physical adsorption of the DEABT on the corroding aluminum surface.<sup>(45, 46)</sup>

Plots of  $\ln(\text{corrosion rate})$  vs.  $1/T$  for 6061 Al composite in 0.5 M sulfuric acid in the absence and the presence of different concentrations of DEAB are shown in Figure 5. As shown in the figure, straight lines were obtained according to Arrhenius – type equation:

$$\ln(\text{corrosion rate}) = A - \frac{E_a}{2.303 RT} \quad (9)$$

where A is a constant, which depends on metal type and electrolyte,  $E_a$  is the apparent activation energy, R is the universal gas constant and T is the absolute temperature. Similar plots were obtained for the base alloy also.

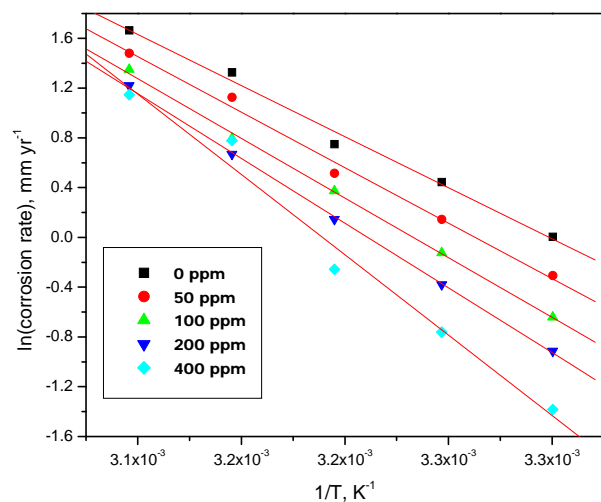


**Figure 5.** Arrhenius plots for the corrosion of composite in 0.5 M H<sub>2</sub>SO<sub>4</sub> at 30 °C in presence of different concentrations of DEABT.

4-(*N,N*-Diethylamino)benzaldehyde thiosemicarbazone as Corrosion Inhibitor for 6061 Al – 15 vol. pct. SiC(*p*) Composite and its Base alloy

Plots of  $\log(\text{corrosion rate}/T)$  vs  $1/T$  for the composite in 0.5 M sulfuric acid in the absence and presence of different concentrations of DEABT are shown in Figure 6. As shown in the Figure, straight lines were obtained according to transition state equation:

$$\text{Corrosion rate} = \frac{RT}{Nh} e^{\frac{\Delta S^\ddagger}{R}} e^{\frac{-\Delta H^\ddagger}{RT}} \quad (10)$$

where  $h$  is Planck's constant,  $N$  is Avogadro's number,  $\Delta H^\ddagger$  is the activation enthalpy and  $\Delta S^\ddagger$  is the activation entropy.

The calculated values of apparent activation energy,  $E_a$ , activation enthalpies,  $\Delta H^\ddagger$ , and activation entropies,  $\Delta S^\ddagger$  for the composite and the base alloy are given in Table 5 and Table 6, respectively. These values indicate that the presence of inhibitor

increases the activation energy,  $E_a$ , and the activation enthalpy,  $\Delta H^\ddagger$ .

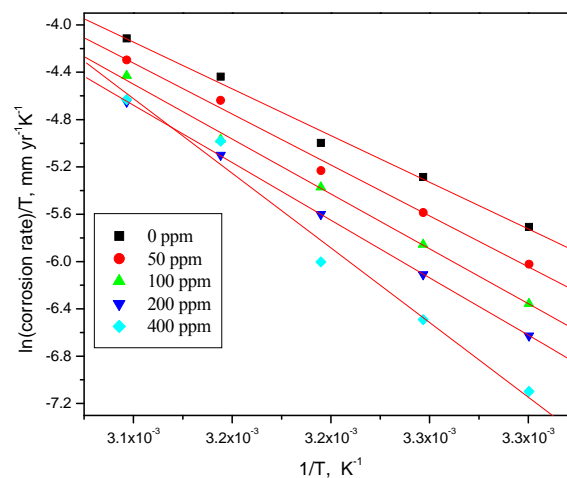


**Figure 6.** Plots of  $\ln(\text{corrosion rate})/T$  vs  $1/T$  for the composite in 0.5 M  $\text{H}_2\text{SO}_4$  at 30 °C in the presence of different concentrations of DEABT.

**Table 5.** Activation parameters for the corrosion of 6061 Al-SiC composite in the presence of different concentrations of DEABT.

Activation parameters	Medium													
	0.5 M $\text{H}_2\text{SO}_4$					0.25 M $\text{H}_2\text{SO}_4$					0.05 M $\text{H}_2\text{SO}_4$			
	Inhibitor concentration (ppm)					Inhibitor concentration (ppm)					Inhibitor concentration (ppm)			
	0	50	100	200	400	0	25	50	100	200	0	10	25	50
$E_a$ (kJ mol <sup>-1</sup> )	68.3	74.1	79.8	86.6	107.3	71.7	80.5	82.7	83.9	86.6	72.4	74.9	75.6	79.5
$\Delta H^\ddagger$ (kJ mol <sup>-1</sup> )	65.6	71.5	77.2	80.9	104.8	69.1	77.9	80.1	81.3	84.0	69.4	72.3	72.8	76.9
$\Delta S^\ddagger$ (J K <sup>-1</sup> mol <sup>-1</sup> )	-23.3	-12.5	4.1	88.1	106.4	-24.1	2.4	6.7	12.5	16.6	-5.8	-2.4	-1.7	15.8

**Table 6.** Activation parameters for the corrosion of 6061 Al base alloy in the presence of different concentrations of DEABT.

Activation parameters	Medium													
	0.5 M $\text{H}_2\text{SO}_4$					0.25 M $\text{H}_2\text{SO}_4$					0.05 M $\text{H}_2\text{SO}_4$			
	Inhibitor concentration (ppm)					Inhibitor concentration (ppm)					Inhibitor concentration (ppm)			
	0	25	50	100	200	0	10	25	50	100	0	5	10	25
$E_a$ (kJ mol <sup>-1</sup> )	63.4	71.0	76.2	76.8	77.6	69.2	76.8	77.3	77.9	78.2	71.7	84.7	86.6	90.9
$\Delta H^\ddagger$ (kJ mol <sup>-1</sup> )	60.8	68.4	73.6	73.9	75.3	66.6	74.3	75.0	75.3	75.6	68.4	82.1	84.0	88.3
$\Delta S^\ddagger$ (J K <sup>-1</sup> mol <sup>-1</sup> )	-58.2	-35.7	-31.5	-20.8	-21.6	-44.0	-30.8	-21.6	-19.1	-18.2	-16.6	0.83	4.9	17.4

The values of  $\Delta S^\ddagger$  are higher for inhibited solutions than that for the uninhibited solutions. This suggested that an increase in randomness occurred on going from reactants to the activated complex. This might be the results of the adsorption of organic inhibitor molecules from the acidic solution which could be regarded as a quasi-substitution process between the organic compound in the aqueous phase and water molecules at electrode surface.<sup>(47)</sup> In this situation, the adsorption of organic inhibitor is accompanied by desorption of water molecules from the surface. Thus the increasing in entropy of activation is attributed to the increasing in solvent entropy.<sup>(48)</sup>

### Adsorption Isotherm

In order to understand the mechanism of corrosion inhibition, the adsorption behavior of the organic adsorbate on the aluminum surface must be known. The degree of surface coverage ( $\theta$ ) for different concentrations of inhibitor was evaluated from potentiodynamic polarization measurements. Attempts were made to fit the  $\theta$  values at different concentrations of DEABT into different adsorption isotherms and the best fit was found with the Langmuir adsorption isotherm. The Langmuir adsorption isotherm is represented by the expression,

$$\frac{\theta}{(1-\theta)} = K_{\text{ads}} C \quad (11)$$

where  $K_{\text{ads}}$  is the equilibrium constant of the inhibitor adsorption process and  $C$  is the inhibitor concentration in the solution. A straight line was obtained on plotting  $C/\theta$  against  $C$ , suggesting that the adsorption of the compound on aluminum surface follows Langmuir adsorption isotherm model. These results show that all the linear correlation coefficients ( $R^2$ ) are almost equal to unity and all the slopes are slightly deviated from unity, which indicates a non-ideal simulating and unexpected from Langmuir adsorption

isotherm. They might be the results of the interactions between the adsorbed species on the metal surface.<sup>(49)</sup> The high values of  $K$  for the studied inhibitor indicate the strong adsorption of inhibitor molecules on the alloy surface. Adsorption isotherms in the presence of different concentrations of DEABT, on the surface of 6061 Al- SiC composite in 0.5 M sulfuric acid at different temperatures are shown in Figure 7. Similar plots were also obtained for the base alloy also.

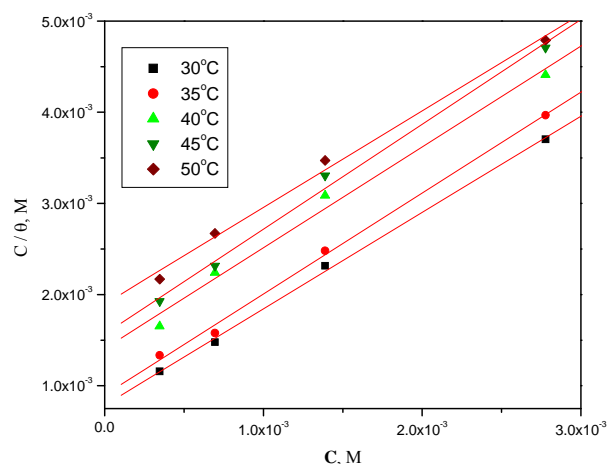


**Figure 7.** Langmuir adsorption isotherms for the adsorption of DEABT on the composite.

The free energy of adsorption,  $\Delta G_{\text{ads}}^0$  was calculated using the relation,

$$\Delta G^0 = -RT \ln \left[ \frac{55.5 \theta}{C(1-\theta)} \right] \quad (12)$$

where  $C$  is the concentration of the inhibitor expressed in mole  $\text{dm}^{-3}$ . The calculated values of  $\Delta G_{\text{ads}}^0$  for DEABT on the composite and the base alloy were in the range of  $-28.28$  to  $-31.26$   $\text{kJ mol}^{-1}$  and  $-26.98$  to  $-32.87$   $\text{kJ mol}^{-1}$ , respectively. The negative values of  $\Delta G_{\text{ads}}^0$  suggest the spontaneous adsorption of DEABT on the composite and the base alloy surfaces. Since the values of  $\Delta G_{\text{ads}}^0$  more negative than  $-40$   $\text{kJ mol}^{-1}$  correspond to chemisorptions and values less negative than  $-20$   $\text{kJ mol}^{-1}$  correspond to physisorption, the obtained values of the  $\Delta G_{\text{ads}}^0$  may be

4-(*N,N*-Diethylamino)benzaldehyde thiosemicarbazone as Corrosion Inhibitor for 6061 Al – 15 vol. pct. SiC(*p*) Composite and its Base alloy

indicative of both physical and chemical process<sup>(50)</sup>.

The enthalpy of adsorption ( $\Delta H_{\text{ads}}^0$ ) and entropy of adsorption ( $\Delta S_{\text{ads}}^0$ ) were calculated using rearranged form of Gibbs – Helmholtz equation

$$\Delta G_{\text{ads}}^0 = \Delta H_{\text{ads}}^0 - T \Delta S_{\text{ads}}^0 \quad (13)$$

The variation of  $\Delta G_{\text{ads}}^0$  with T gives a straight line with a slope that equals  $\Delta S_{\text{ads}}^0$  and intercept equals to  $\Delta H_{\text{ads}}^0$ . The data obtained for the adsorption of DEABT on the aluminum composite and the base alloy are listed in Table 7. The negative sign of  $\Delta H_{\text{ads}}^0$  in sulfuric acid solution indicates that the adsorption of inhibitor molecule is an exothermic process.

**Table 7.** Thermodynamic parameters for the adsorption of DEABT on the Al composite and the base alloy in 0.5 M sulfuric acid at different temperatures.

Temperature	Composite				Base alloy			
	K	$\Delta G_{\text{ads}}^0$	$\Delta H_{\text{ads}}^0$	$\Delta S_{\text{ads}}^0$	K	$\Delta G_{\text{ads}}^0$	$\Delta H_{\text{ads}}^0$	$\Delta S_{\text{ads}}^0$
(K)	(M <sup>-1</sup> )	(kJ mol <sup>-1</sup> )	(kJ mol <sup>-1</sup> )	(J mol <sup>-1</sup> K <sup>-1</sup> )	(M <sup>-1</sup> )	(kJ mol <sup>-1</sup> )	((kJ mol <sup>-1</sup> )	(J mol <sup>-1</sup> K <sup>-1</sup> )
303	1270.6	-29.10			1631.3	-28.8		
308	1112.3	-28.30			1497.0	-28.5		
313	709.2	-27.30	-64.0	-116.0	1400.5	-28.4	-54.8	-92.3
318	636.9	-26.90			1257.9	-27.5		
323	526.3	-26.90			970.8	-27.0		

Generally, an exothermic adsorption process signifies either physisorption or chemisorptions, while endothermic process is attributable to chemisorptions.<sup>(51)</sup> Typically, the enthalpy of physisorption process is lower than that 41.86 kJ mol<sup>-1</sup> while the enthalpy of chemisorptions process approaches 100 kJ mol<sup>-1</sup>.<sup>(52)</sup> In the present study, the absolute value of enthalpy is -64.01 kJ mol<sup>-1</sup> and -54.80 kJ mol<sup>-1</sup> for the composite and the base alloy, respectively, which is an intermediate case. The  $\Delta S_{\text{ads}}^0$  values in the presence of inhibitor are large and negative, indicating a decrease in disordering on going from reactants to metal adsorbed species<sup>(50)</sup>.

### Effects of Acid Concentration.

Table 5 lists the maximum attainable inhibition efficiency on the composite in sulfuric acid of different concentrations. As observed from the table, the inhibition efficiency increases with the increase in

sulfuric acid concentration and is maximum in 0.5 M sulfuric acid solution. The increase in the extent of adsorption of the inhibitor on the alloy surface and in turn the increase in the inhibitor efficiency can be attributed to the following two facts:

The increase in the concentration of the acid increases the extent of protonation of the inhibitor molecules, thereby facilitating their adsorption on the cathodic sites.

With the increase in the concentration of the acid, the anion of the acid (SO<sub>4</sub><sup>2-</sup>) adsorb physically on the positively charged metal surface, giving rise to a net negative charge on the metal surface.<sup>(40)</sup> This further facilitates the adsorption of protonated inhibitor molecules.

### Effect of The Immersion Time

Electrochemical impedance spectroscopy is a useful technique for long time tests, because they do not significantly disturb the system and it is possible to follow it overtime.<sup>(53)</sup> Immersion time experiments in the present work were carried out in different concentrations of sulfuric acid containing 400 ppm of inhibitor for 360 min and Nyquist plots were recorded every 5min during the initial 30 min, and then every 30 min afterward. The results obtained (not shown here) showed that the immersion time has a great influence on the size and shape of the impedance spectra, and therefore the inhibition efficiency of the inhibitor. The capacitive loop was found to increase in size with the increase of immersion time, reaching a maximum in 30 min and remained fairly constant afterward. More details are shown in Figure 8, which represents the variation of both  $R_p$  and  $C_{dl}$  with the immersion time recorded for DEABT in 0.5 M sulfuric acid solution. It is obvious from Figure 8, that the  $R_p$  values increase from 378.9 to 506.7  $\Omega \text{ cm}^2$  during the initial 30 min and remain fairly constant afterward. The inhibition efficiency increases from 75 % to 80 %. At the same time, the capacitance values are reduced drastically from 117 to 65  $\mu\text{F cm}^{-2}$  during the initial 30 min and remained fairly constant afterward. This means that the formation of the inhibitor surface film, and therefore the inhibitor adsorption, on the electrode surface is fast and gets completed within 30 min. These results demonstrate that the inhibition efficiency increases with the increase in immersion time. It is possible that with increasing immersion time and concentration, a compact adsorbed film of the inhibitor is formed on the aluminum surface, since adsorption of more DEABT is facilitated on the aluminum surface. The formation of such adsorbed film is confirmed by EDX examinations of the electrode surface.

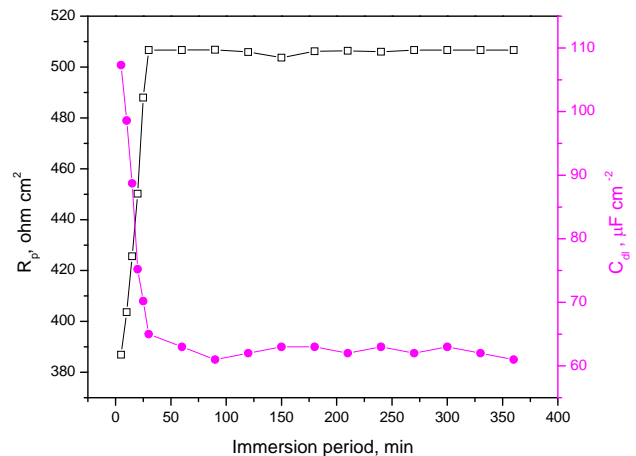


**Figure 8.** Dependence of  $R_p$  and  $C_{dl}$  on the immersion time for the corrosion of Al composite in 0.5M sulfuric acid solution.

### Mechanism of Inhibition

The corrosion inhibition property of DEABT through adsorption on the surface of the composite or the base alloy can be attributed to the presence of electronegative elements like nitrogen and sulfur and also to the presence of  $\pi$  electrons on the benzene ring. The metal surface in contact with a solution is charged due to the electric field that emerges at the interface on the immersion in the electrolyte. This can be determined, according to Antrapov<sup>(54)</sup> by comparing the zero charge potential and the rest potential of the metal in the corresponding medium. The value of  $\text{pH}_{Z_{ch}}$ , which is defined as the pH at a point of zero charge is equal to 9.1 for aluminum.<sup>(55)</sup> So aluminum is positively charged in highly acidic medium, as the ones used in this investigation. Therefore, sulfate ions and DEABT can be adsorbed on the aluminum surface via their negative centres. Also, DEABT can be protonated in the highly acidic solution used in the investigation. The mechanism of adsorption of protonated DEABT can be predicted on the basis of the mechanism proposed for the corrosion of aluminum in hydrochloric acid.<sup>(56)</sup> According

*4-(N,N-Diethylamino)benzaldehyde thiosemicarbazone as Corrosion Inhibitor for 6061 Al – 15 vol. pct. SiC(p) Composite and its Base alloy*

to this mechanism, anodic dissolution of Al follows steps.



The cathodic hydrogen evolution is according to the following steps



In acidic solution, all the nitrogen atoms including secondary amino group can be protonated easily because they are all planar and having greater electron density Figure 9. The protonated molecules can adsorb on the cathodic sites of aluminum in competition with the hydrogen ions (equation 16). Co-ordinate covalent bond formation between electron pairs of unprotonated S atom and metal surface can take place. Further, DEABT molecules are chemically adsorbed due to the interaction of  $\pi$ -orbitals with metal surface following deprotonation step of the physically adsorbed protonated molecules.

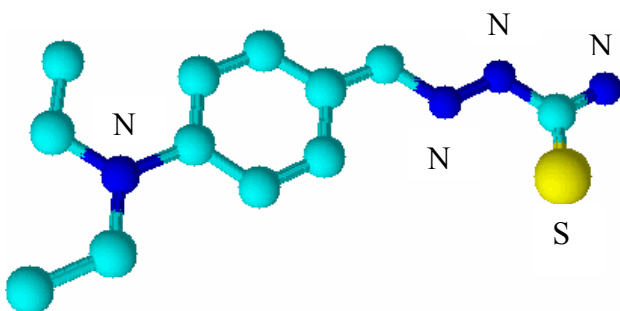


**Figure 9.** Three dimensional representation of DEABT molecule.

In the present case, the value of  $\Delta G_{\text{ads}}^0$  is  $-31.26 \text{ kJ mol}^{-1}$  to  $-32.87 \text{ kJ mol}^{-1}$ ,

indicates that adsorption of DEABT on the surface of aluminum involves both physical and chemical process. But, as it can be seen from Table 7, the value of  $\Delta G_{\text{ads}}^0$  decreases with the increase in temperature, indicating that the adsorption of DEABT is not favored at higher temperatures. This implies that DEABT is adsorbed predominantly by physisorption on the surface of aluminum composite.

In order to gain the information about the surface composition of the composite and the base alloy, EDX studies were carried out on samples which were exposed to the corrosion medium in the presence and absence of the inhibitor. EDX spectra of the composite sample exposed to the sulfuric acid corrosion medium in the absence of inhibitor showed spectral lines corresponding to aluminum, silicon, oxygen and small peaks corresponding to sulfur. The samples exposed to corrosion medium in the presence of inhibitors showed additional carbon, nitrogen and sulfur signals, indicating surface coverage by the inhibitor. Presence of higher percentage of carbon, nitrogen and sulfur on the surface of the composite samples than on base alloy reveals the higher adsorption of DEABT on the composite than on the base alloy. This also accounts for higher inhibition efficiency achieved on composite sample than on the base alloy sample.

## Conclusions

1. DEABT acts as a good corrosion inhibitor for 6061 Al- 15 vol. pct. SiC<sub>(p)</sub> composite and the base alloy in sulfuric acid medium.
2. Corrosion inhibition efficiency of DEABT increases with the increase in the concentration of inhibitor up to a critical concentration.
3. DEABT behaves as a cathodic type inhibitor.

4. Inhibition efficiency of DEABT on Al composite is more than that on the base alloy.

5. Inhibition efficiency of DEABT on the aluminum composite and the base alloy increases with the increase in concentration of sulfuric acid and decreases with the increase in temperature from 30 °C - 50 °C.

6. Inhibitor obeys Langmuir's model of adsorption and the adsorption is predominantly through physisorption.

## References

1. Sanders, Jr., T. H. and Starke, Jr., E. A. (1989). *Proc. 5<sup>th</sup> Int. Conf. on 'Al – Lithium alloys'*. Materials & Composites Engineering Publications. Birmingham, UK: 1-40.
2. Monticelli, C., Zucchi, F., Brunoro, G. and Trabanelli, G. (1997) Corrosion and corrosion inhibition of alumina particulate aluminium alloys metal matrix composites in neutral chloride solutions. *J. Appl. Electrochem.* **27(3)**: 325-334
3. Pardo, A., Merino, M. C., Merino, S., Viejo, F., Carboneras, M. and Arrabal, R. (2005) Influence of reinforcement proportion and matrix composition on pitting corrosion behaviour of cast aluminium matrix composites (A3xx.x/SiCp). *Corros. Sci.* **47**:1750-1764
4. Da Costa, C. E., Velasco, F. and Toralba, J. M. (2000). *Rev. Metal. Madrid*, **36**, 179.
5. Rohatgi, P. K. (1991). *JOM.* **43**: 10.
6. Pardo, A., Merino, M.C., S., Lopez, M. D., Viejo, F. and Carboneras, M. (2003). *Mater. Corros.* **54**: 311.
7. Peel, C. J., Moreton, R., Gregson, P. J. Hunt, E.P. (1991). *Proc. XIII Int. Conf on 'Society of advanced material and process engineering.* SAMPE, Covina, CA:189.
8. Hutchings, I. M., Wilson, S., Alpas, A.T. and Clyne, T. W. (2000). *Comprehensive composite materials.* Vol.3, Elsevier Science. UK. : 501.
9. Aylor, D. M. (1987) Corrosion of Metal Matrix Composites. In: *Metals Handbook*, Vol. 13, 9<sup>th</sup> ed. Metals Park, Ohio:ASM International: 859.
10. Trowsdate, A. J., Noble, B., Haris, S. J., Gibbins, I. S. R., Thomson, G.E. and Wood, G.C. (1996). The influence of silicon carbide reinforcement on the pitting behavior of aluminium. *Corros. Sci.* **38**:177.
11. Bentiss, F., Treisnel, M., Lagrence, M. (2000) Inhibitor effects of triazole derivatives on corrosion of mild steel in acidic media. *Br. Corros. J.* **35(4)**:315-320
12. Rao, S.A., Padmalatha, J. Nayak, A. and Shetty, N. (2005) *J. Met. Mater. Sci.* **47**:51.
13. Desai, M. N., Desai, S. M., Gandhi, M. H. and Snaha, C. B. (1971) *Anti - Corros. Meth. Mater.* **18**:19.

4-(N,N-Diethylamino)benzaldehyde thiosemicarbazone as Corrosion Inhibitor for 6061 Al – 15 vol. pct. SiC(p) Composite and its Base alloy

14. Desai, M. N., Rana, S. S., Gandhi, M.H. and Snaha, C. B. (1971). *Anti - Corros. Meth. Mater.* **18**:19.
15. Rama Char, T. L. and Padma, O. K. (1969) *Trans. Inst. Chern. Engrs.* **47**:177.
16. Putilova, I. N., Balezin, S. A. and Arannik, B. (1960). *Metallic Corrosion Inhibitors*. Oxford: Pergamon: 67.
17. Trabaneli, G. Carassiti, V. (1970). *Advances in Corrosion Science and Technology*. New York: Plenum Press :147.
18. Rozerfeld, I. L. (1981) *Corrosion Inhibitors*. New York: Mc Graw Hill: 147.
19. Nathan, C.C.(1973). *Corrosion Inhibitors*. Houston: NACE : 7.
20. Hunkeler, F. And Bohni, H.(1983). *Workstoffe u. Korrasion*. **34**:68.
21. Kuznetsov, Y. J. (1984). *Protection of Metals*. **20**:282.
22. Singh, S., Athar, F. And Azam, A. (2005). Synthesis, spectral studies and in vitro assessment for antimicrobial activity of new cyclooctadiene ruthenium (II) complexes with 5 -nitrothiophene-2-carboxaldehydethiosemicarbazones. *Bioorg Med. Chem.Letter*, **15**: 5424.
23. Abd El- Nabey, B.A. and Khamis, E. (1986). Effect of temperatura on the inhibition of the acid corrosion of steel by benzaldehyde thiosemicarbazone :Impedance measurements. *Surf. Coat. Tech.* **28**:83-91
24. Shah, P. T. and Daniels, T. C. (1950). *Rev. Trav. Chim.* **69**:1545.
25. Bethencourt, M., Botana, F. J., Cauqui, M. A., Marcos, M. and Rodriguez, M. A. (1997). *Alloys Compd.* **250**:455.
26. Abdel Rahim, S. S., Hassan H. H. and Amin M. A. (2002). *Mater. Chem. Phys.* **78**:337.
27. Aramaki, K. (2001). Effects of organic inhibitors on corrosion of zinc in an aerted 0.5 M NaCl solution. *Corros. Sci.* **43**:1985.
28. Abdl Aal, M. S., Radwan, S. and Saied, A. El. (1983). *Br. Corr. J.* **18**:102.
29. Khaled, K. F. and Al-Qahtani, M. M., (2009). *Mater.Chem. Phys.* **113**:150.
30. Abdel Rehim, S. S., Hamdi Hassan,H.H. and Amin, M.A.(2002). Corrosion and corrosion inhibition of AI and some alloys in sulphate solutions containing halide ions investigated by an impedance technique. *App. Surf. Sci.* **187**: 279-290.

31. Lenderink, H. J. W., Linden, M. V. D. and Dewit, J. H. W. (1993). Corrosion of aluminium in acidic and neutral solutions. *Electrochim. Acta* **38**:1989.
32. Wit, J. H. W. and Lenderink, H. J. W. (1996). Electrochemical impedance spectroscopy as a tool to obtain mechanistic information on the passive behaviour of aluminium. *Electrochim. Acta* **41**:1111-1119.
33. Bessone, J. B., Salinas, D. R., C., Mayer Ebert, M. and Lorenz, W. J. (1992). An EIS study of aluminium barrier-type oxide films formed in different media. *Electrochim. Acta*. **37**: 2283-2290.
34. Frers, S. E., Stefenel, M. M., Mayer, C. and Chierchie, T. (1990). *J. Appl. Electrochem.* **20**:996.
35. Metikos-Hukovic, M., Babic, R. and Grubac, Z. (1998). Corrosion protection of aluminium in acidic chloride solutions with nontoxic inhibitors. *J. Appl. Electrochem.* **28**:433.
36. Brett, C. M. A. (1990). *J. Appl. Electrochem.* **20**:1000.
37. Lee, E. J. and Pyun, S.I. (1995). The effect of oxide chemistry on the passivity of aluminium surfaces. *Corros. Sci.* **37**:157-168.
38. Brett, C.M.A. (1992). On the Electrochemical behaviour of aluminium in acidic chloride solution. *Corros. Sci.* **33**:203.
39. Khaled, K. F. and Al-Qahtani, M. M., (2009). *Mater. Chem. Phys.* **113**:150.
40. Ehteram, N. A. (2009). *Mater. Chem. Phys.* **114**:533.
41. Aytac, A., Ozmen, U., Kabasakaloglu, M. (2005). *Mater. Chem. Phys.* **89**:176.
42. Mansfeld, F., Lin, S., Kim K. and Shih, H. (1987). Pitting and surface modification of SiC/Al. *Corros. Sci.* **27**:997.
43. Mansfeld, F., Lin, S., Kim, S. and Shih, H. (1988). *Mater. Corros.* **39**:487.
44. Migahed, M. A. (2005). *Mater. Chem.* **93**:48.
45. Abdallah, M. (2004). Antibacterial drugs as corrosion inhibitors for corrosion of aluminium in hydrochloric solution. *Corros. Sci.* **46**:1981.
46. Oguzie, E. E. (2007). Corrosion inhibition of aluminium in acidic and alkaline media by *Sansevieria trifasciata* extract. *Corros. Sci.* **49**:1527-1539.
47. Sahin, M., Bilgic S. and Yilmaz, H. (2002). *Appl. Surf. Sci.* **195**:1.
48. Ateya, B. G., El-Anadouli, B. E. and El-Nizamy, F.M. (1984). The adsorption of thiourea on mild steel. *Corros. Sci.* **24**:509-515.

*4-(N,N-Diethylamino)benzaldehyde thiosemicarbazone as Corrosion Inhibitor for 6061 Al – 15 vol. pct. SiC(p) Composite and its Base alloy*

49. Tao, Z., Zhang, S., Li, W. and Hou, B. (2009). Corrosion inhibition of mild steel in acidic solution by some oxo-triazole derivatives. *Corros. Sci.* **51**: 2588-2595.
50. Geler, E. and Azambuja, D. S. (2000). Corrosion inhibition of copper in chloridesolutions by pyrrole. *Corros. Sci.* **42**:631-643.
51. Durnie, W., De Marco R., Kinsella B. and Jefferson,A.(1999).*J.Electrochem Soc.* **146**:1751.
52. Martinez, S. and Stern, I. (2002). *Appl. Surf. Sci.* **199**:83.
53. Moretti, G., Guidi, F. and Grion, G. (2004).Tryptamine as a green iron corrosion inhibitor in 0.5 M deaerated sulphuric acid. *Corros.Sci.* **46**:387-403.
54. Antropov, L.I., Makushin, E.M., and Panasenko, V.F. (1981). *Metallic Corrosion Inhibitors*. Kiev, Technika :182.
55. Tschapek, M., Wasowski, C. and Sanchez, R.M.T.(1976).*J.Electroanal. Chem.* **74**:167.
56. Awady, A.A., Abd, B.A. El- Nabey, S. and Aziz, G. (1993). *J. Chem. Soc. Faraday Trans.* **84**:795.